UKAEA-CCFE-PR(21)80

Peng Shi, Hongjuan Sun, Ge Zhuang, Zhifeng Cheng, Li Gao, Zhipeng Chen, Jingchun Li, Yinan Zhou, the J-TEXT Team

Observation of the high-field-side high-density front in J-TEXT tokamak

Observation of the high-field-side high-density front in J-TEXT tokamak

Peng Shi, Hongjuan Sun, Ge Zhuang, Zhifeng Cheng, Li Gao, Zhipeng Chen, Jingchun Li, Yinan Zhou, the J-TEXT Team

This is a preprint of a paper submitted for publication in Plasma Physics and Controlled Fusion

Observation of the high-field-side high-density front in J-TEXT tokamak

Peng Shi[1,2,3], Hongjuan Sun[1], Ge Zhuang[4*], Zhifeng Cheng[3], Li Gao[3], Zhipeng Chen[3], Jingchun Li[5], Yinan Zhou[3], Chengxi Zhou[3] and the J-TEXT Team

[1]United Kingdom Atomic Energy Authority, Culham Centre for Fusion Energy, Culham Science Centre, Abingdon, Oxon, OX14 3DB, United Kingdom

[2]Southwestern Institute of Physics, PO Box 432, Chengdu 610041, China

[3]International Joint Research Laboratory of Magnetic Confinement Fusion and Plasma Physics, State Key Laboratory of Advanced Electromagnetic Engineering and Technology, School of Electrical and Electronic Engineering, Huazhong University of Science and Technology, Wuhan 430074, China

[4]School of Physical Sciences, University of Science and Technology of China, Hefei, Anhui 230026, China

[5]Department of Earth and Space Sciences, Southern University of Science and Technology, 518055 Shenzhen, Guangdong, People's Republic of China

[*]Corresponding author: gezhuang@ustc.edu.cn & peng.shi@ukaea.uk

This article reports the first observation of the high-field side high density (HFSHD) front in limiter devices, which sheds a new light on understanding this phenomenon, originally observed on divertor tokamak. In the J-TEXT high density discharges, the high-density front at the HFS scrape-off layer (SOL) region has been clearly identified by the far-infrared laser polarimeter-interferometer. The HFSHD front forms at the HFS SOL when the plasma density reaches a critical value, and then expands poloidally while propagating into the main plasma region as the density further increases. Usually, a well-developed HFSHD front is found to evolve from the stable state of staying at HFS edge to the dynamic state of moving poloidally, while approaching to density limit. It is found that both the density threshold of HFSHD front formation and the maximum density of the region itself increase with I_P. Furthermore, the maximum achievable density on J-TEXT seems to be correlated with the evolution of the HFSHD front, suggesting that the region may play a role in setting the operational limit on J-TEXT. The observation suggests that considering the existence of the HFSHD front in simulations should not be limited to single null divertor devices and additional mechanisms may need to be considered to explain its formation and development.

1. Introduction

In order to keep the power and particle load on plasma facing components below material limits, operation under partially or completely detached condition is highly desired for the next-step tokamaks [1], such as the International Thermonuclear Experimental Reactor (ITER) [2] and Chinese Fusion Engineering Testing Reactor (CFETR) [3]. During studies of tokamak plasma under detached conditions, a so-called high-field side high-density (HFSHD) front has been observed on AUG and JET [4–7]. In these studies, when the inner divertor is detached while the outer divertor stays attached, a poloidally localized high-density region occurs in the HFS SOL which extends from X-point towards the HFS midplane [5]. This region is known as the HFSHD front. Simulations with SOLPS show that the HFSHD front plays an important role in the fuelling of core plasma and thus can lead to strong change in global performance [7]. Dedicated experiments on AUG have shown evidence that the HFSHD front can significantly influence the density profile position relative to separatrix [8]. Further, experiments and modeling have discovered that the shift of density profile has an impact on pedestal stability and subsequently on plasma confinement [8–11]. Thus, understanding the underlying physics of the HFSHD front and its correlation with detachment is important for the operation of future machines.

Recently, the HFSHD front has been also recorded in J-TEXT tokamak, which is the first observation on limiter devices. The paper reports the characteristics of the HFSHD front on J-TEXT and compares the results with those on divertor machines. The results on a limiter machine shed a new light on understanding the phenomena. The rest of the paper is organized as follows: Section 2 describes the experimental setup and main diagnostics for the investigation of the HFSHD front in the J-TEXT tokamak; Section 3 presents the observations which clearly show the formation and development of the HFSHD front in density ramping discharges; Section 4 gives the influences of the global plasma current and edge plasma parameters on the properties of HFSHD front; Section 5 provides the summary and disccusion.

2. Experimental Setup

The J-TEXT tokamak (formerly TEXT-U [12]) is a conventional medium-sized tokamak with a major radius of $R_0 = 1.05\ m$ and minor radius of $a = 0.25 - 0.29\ m$ (set by the silicon-carbide coated graphite limiter). The first wall and the limiter are covered with carbon tiles. Therefore, the dominating impurity in the J-TEXT is carbon. The discharges are performed with Ohmic heating and the working gas is hydrogen. Continuous gas-puffing is used to raise the plasma density in a single shot. In the experiments, the plasma parameters are $I_P = 120 - 170\ kA, B_T = 1.7 - 2.1\ T, q_a = 4 - 5.5, a = 0.255\ m$. The maximum density in J-TEXT Ohmic plasma is well below the Greenwald density, near $0.7n_G$, where n_G is the Greenwald density equal to $I_P/(\pi a^2)$ with I_p in units of MA and a in units of metres. Fig. 1 depicts the main diagnostics used to record the formation and evolution of the HFSHD front in J-TEXT. The line-integrated electron density is measured by a 17-channel far-infrared laser polarimeter-interferometer system (POLARIS) [13], which views the plasma vertically at intervals of 3 cm on the radial mid-plane from $r = -24\ cm$ to $r = +24\ cm$ and covers the plasma poloidal cross-region from $-0.94a$ to $0.94a$, where $r = R - R_0$. Here, $r < 0$ and $r > 0$ corresponds to high-field-side (HFS) and low-field-side (LFS), respectively. A 26-channel photodiode array (PDA) system is used to measure the line emission of carbon III (C_{III}) at the wavelength of 465 nm. As similar to POLARIS, the C_{III} array also covers both the HFS and LFS of the tokamak. The inner-most three chords — emphasized in Fig. 1 — view the region where the HFSHD front is located. In addition, J-TEXT has a CCD camera system which measures the visible emission distribution with a temporal resolution of 5 ms.

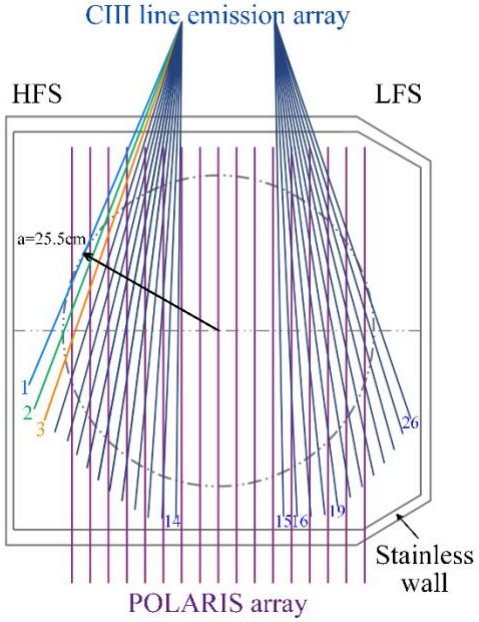

Figure 1. Viewing lines of the J-TEXT photodiode array (PDA) (in blue color) and polarimeter-interferometer system (POLARIS) (in magenta color), respectively.

3. Experimental observation of the HFSHD front in high density plasma

The temporal traces for a typical density-ramp discharge with a HFSHD front is shown in Fig. 2. The discharge has $I_P = 170\ kA, B_T = 2.1\ T, q_a = 3.9$. The speed of gas-puff fueling was constant during the current flat-top. A density limit disruption occurs at $t = 545\ ms$ and the maximum central line-average density is $\bar{n}_{e0} = 5.4 \times 10^{19}\ m^{-3} = 0.65n_G$. During the interval of $250\ ms < t < 540\ ms$, the central (at $r = 0\ cm$) line-average electron density increases steadily (Fig. 2(c)). The line-average density at $r = -24\ cm$ (very edge of HFS) also increases throughout this period, but there is a rise in its rate of increase from about $t = 400\ ms$. The line-average density at the very edge on the LFS ($r = 24\ cm$) changes little throughout the same period, as shown in (Fig. 2(d)). Concomitantly, the C_{III} emission at the

HFS edge also increases, as indicated in Figs. 2(e). This shows that a local high-density plasma region has formed in the HFS SOL as the plasma density exceeds a critical value ($n_{crit} = 4.6 \times 10^{19}\ m^{-3}$ in this discharge). Such observations characterize the typical features of the HFSHD front phenomenon, as described in Refs.[6,7]. In addition, the location and evolution of the HFSHD front were recorded by the visible CCD camera, as shown in Fig. 2(f). The dotted circle in Fig. 2(f) denotes the last closed flux surface (LCFS), determined by the position of the limiter. Before the onset of the HFSHD front ($t = 300\ ms$), the visible line radiation at the plasma boundary is very weak and approximately symmetric. However, after the formation of the HFSHD front ($t = 440\ ms$), a bright spot appears on the HFS of the midplane, located mainly outside the LCFS. Moreover, by comparing the CCD films at $440\ ms$ and $500\ ms$, it is seen that the bright spot expands poloidally and moves into the main plasma as the density further increases. Clearly, the location of the bright spot on the visible CCD film corresponds to the region of the HFSHD front. Thus, the CCD picture is a favorable instrument to study the evolution and movement of the HFSHD front.

Fig. 3 shows profiles of the line-average electron density (Fig. 3(a)) and line-integral C_{III} emission intensity (Fig. 3(b)) during the HFSHD front formation, measured with the diagnostics and lines of sight shown in Fig. 1. During the interval of $400\ ms < t < 530\ ms$, the electron density at the HFS edge increases significantly, while that in the other channels varies little. This indicates that the HFSHD front is highly localized in the inner, HFS region, and the bulk of the confined plasma ($r > -20\ cm$) remains almost unchanged. At the final stage of the discharge, the line-average density across the HFSHD front ($r = -24\ cm$) reaches $4 \times 10^{19}\ m^{-3}$, which is four times higher than that of the LFS region and almost comparable to the central density. In some cases, the density at the HFS edge has been observed to be almost a factor of 10 larger than the density just outside the LCFS.

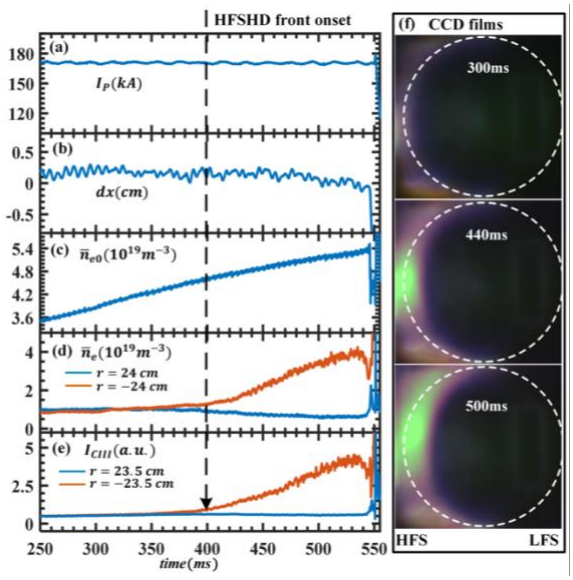

Figure 2. Time evolution of the main parameters for a typical discharge (#39669) of density ramping to limit disruption in J-TEXT, indicating that the HFSHD front occurs at $400\ ms$. (a) Total plasma current, (b) Horizontal plasma displacement, (c) Central line-average electron density, (d) Line-average electron density at the most HFS and LFS edge measured by POLARIS, (e) Line emission of CIII measured by PDA, (f) Visible CCD camera films, where the dotted circles denote the LCFS.

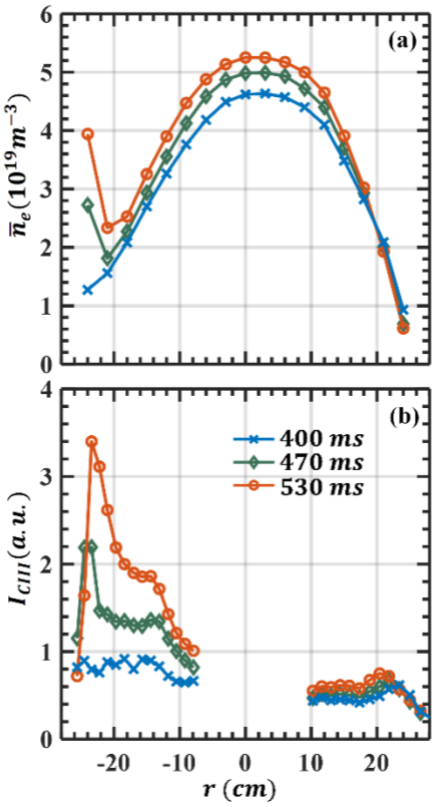

Figure 3. Corresponding to Fig. 2, time evolution of the radial distributions of (a) line-average electron density measured by POLARIS, and (b) line-integral C_{III} radiation intensity obtained by the PDA array.

More details of the evolution of the HFSHD front with continuous increase of the density, is illustrated in Fig. 4. The three inner-most channels of the C_{III} emission and electron density are plotted in Fig. 4(a) and (b) respectively. Fig. 4(c) shows six visible CCD pictures, which corresponds to the six points in Fig. 4(b), indicated by arrows on the X-axis. Little emission is observed at the first point ($\bar{n}_{e0} = 3.8 \times 10^{19}\ m^{-3}$), whereas the HFSHD front is obvious at the third point ($\bar{n}_{e0} = 4.9 \times 10^{19}\ m^{-3}$). Interestingly, at the second point ($\bar{n}_{e0} = 4.5 \times 10^{19}\ m^{-3}$), the HD front is not seen on POLARIS, but a luminous spot can already be observed with the CCD in the HFS SOL. This indicates that the HFSHD front initially forms in the SOL.

The evolution of the HFSHD front can be divided into two different phases with the continuous increase of density. The first phase is given the name 'growing phase'. At this phase, the HD front is localized at the HFS edge while its magnitude grows. From CCD images 2-4 in Fig. 4 (c), it is seen that the HFSHD front stays at the very edge of HFS during this phase. Meanwhile, its extent expands mainly along the poloidal direction. The process is confirmed by the variation of the C_{III} emission and electron density at the HFS edge in Fig. 4(a) and (b). Both the inward shift of the peak of the C_{III} emission from channel 1 (CH1) to channel 3 (CH3) and the time delay of the occurrence of the electron density nonlinear arising from $-24\ cm$ to $-18\ cm$, are well explained by the growth and expansion of the HFSHD front. At the second phase, as the high-density front reaches a critical value ($\bar{n}_{e0} = 5.4 \times 10^{19}\ m^{-3}$), the HFSHD front is found to quickly move poloidally, as can be seen in CCD images $5 \rightarrow 6$ in Fig. 4(c). The start-up of this poloidal movement can be identified by the roll-over of the electron density and C_{III} emission at the HFS edge, as shown in ⑤ →⑥ of Fig. 4(a) and Fig. 4 (b). The second phase is thus named as the 'moving phase'.

The above features comprise the typical characteristic of HFSHD front on J-TEXT. It is a common phenomenon in J-TEXT high density plasmas and the critical density threshold for the occurrence of the HFSHD front is well below that of the Greenwald density limit. During the initial 'growing phase', the HFSHD front is quite stable at the HFS edge and will remain constant if the plasma density remains unchanged. The front can disappear if the plasma density backwards decreases down to the critical threshold. The poloidal movement of the HFSHD front during the subsequent 'moving phase' is quite rapid, which can be inferred by the step-like drop of the electron density at $r = -24\ cm$. The

macro-MHD instability and density limit disruption usually occurs during the 'moving phase' of the HFSHD front. It seems that the movement of the HFSHD front deteriorates plasma confinement rapidly.

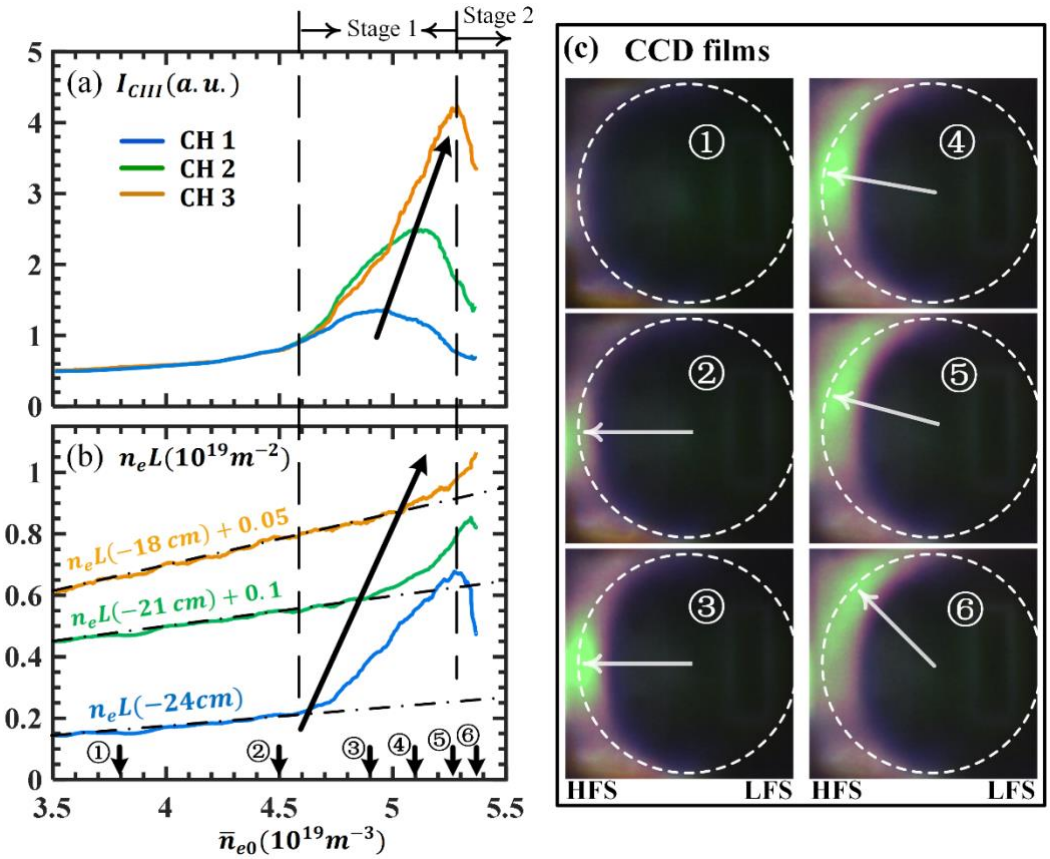

Figure 4. Corresponding to Fig. 2, traces of the three inner-most chords of (a) C_{III} emission and (b) line-integral electron density with the central line-average electron density. (c) Visible CCD camera films at six-time pieces corresponding to the black arrows on the X-axis of Fig. 2 (b). The dotted circles denote the LCFS.

4. The role of plasma parameters on the formation of the HFSHD front

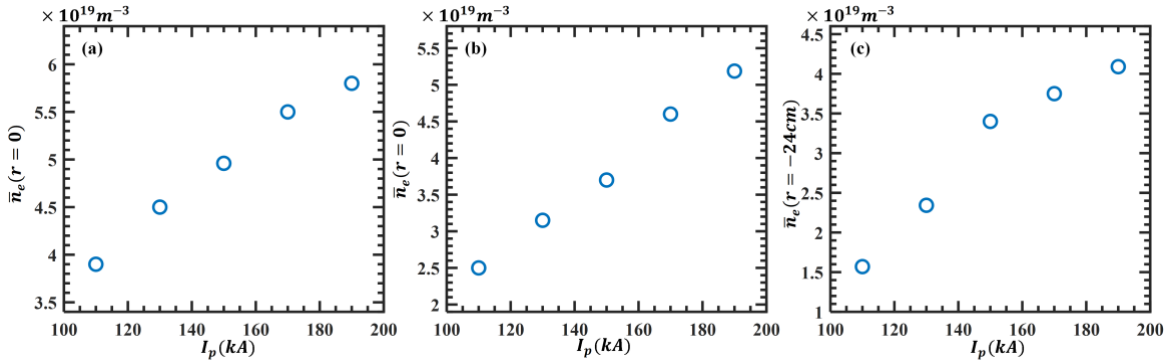

Figure 5. For a set of similar discharges with varying plasma current, the critical central line-average density at (a) the occurrence of the density limit disruption; and (b) the HFSHD front plotted against the total plasma current. (c) The maximum density of the HFSHD front, represented by most inner edge line density, against the total plasma current for the same discharges.

Fig. 5 (a) and (b) summarize the maximum achievable density from density limit (DL) discharges on J-TEXT and the threshold density of HFSHD front formation in the discharges, with different plasma current (I_P) and the same toroidal magnetic field (B_T) on J-TEXT. For the maximum achievable density ($\bar{n}_{e0,DL}$), the experimental data from J-TEXT agrees well with the Greenwald scaling law [14], which means that the density limit has a linear relationship with I_P (Fig. 5(a)). The density limit at higher current is a little lower than would be expected from the linear relationship. This may be due to the enhanced MHD activity observed in $q_a < 4$ plasmas on the J-TEXT tokamak,

which has been reported in Ref. [15]. The threshold density for the appearance of the HFSHD front ($\bar{n}_{e0,thres}$) is observed to have a similar linear dependence on I_P. Here, the time of appearance of the HFSHD front is measured as that when there is rise in the rate of change of increase of HFS edge electron density. For instance, in the plasma shown in Fig. 4, $\bar{n}_{e0,thres}$ is $4.6 \times 10^{19}\ m^{-3}$. The similar $\bar{n}_{e0,thres}$~I_P and $\bar{n}_{e0,DL}$~I_P relationships suggest that the HFSHD front might play an important role in setting the maximum achievable density on J-TEXT. In addition, as shown in Fig.5 (c), the local maximum density at the HFSHD front ($n_{e,HFSHD}$), which is indicated by the line-average density at $r = -24\ cm$, increases with I_P as well. That is consistent with the experimental observations on ASDEX-U, where the density value of the HFSHD front increases with the heating power and plasma current [15,16]. However, the relationship between $n_{e,HFSHD}$ and I_P is not quite linear. The density of the HFSHD front tends to be saturated after I_P exceeds $150\ kA$.

Fig.6 (a) presents the average edge electron density at the onset of the HFSHD front ($\bar{n}_{e\_edge,thres}$) versus total plasma current. In order to exclude the influences of plasma displacement on density measurement, here, the edge electron density is taken as the mean value of line-average densities on the most LFS ($r = +24\ cm$) and HFS ($r = -24\ cm$) chords. The $\bar{n}_{e\_edge,thres}$ increases with total plasma current, which is similar to the $\bar{n}_{e0,thres}$ (showed in Fig.5 (b)). But the difference is, the relationship of $\bar{n}_{e\_edge,thres}$~I_P is quite not as linear as $\bar{n}_{e0,thres}$~I_P. Obviously, the $\bar{n}_{e\_edge,thres}$ increases faster at large I_P region ($> 150kA$), than the low I_P area ($< 150\ kA$). To divide the $\bar{n}_{e0,thres}$ by $\bar{n}_{e\_edge,thres}$, we can obtain a rough peaking factor of density profile at the onset of the HFSHD front. As plotted in Fig.6 (b), the peaking factor of density distribution decreases largely in large I_P region. Combining with the $\bar{n}_{e\_edge,thres}$~I_P relationship, it seems that a more peaked density profile is favorable to the formation of the HFSHD front. Behind the density distribution, the key parameter should be the radial transport. A peaked density profile means small perpendicular transport, and small edge temperature as well. And low enough temperature is one of demanded conditions for HFSHD front formation. This logic can qualitatively explain the non-linear dependence of $\bar{n}_{e\_edge,thres}$ on I_P.

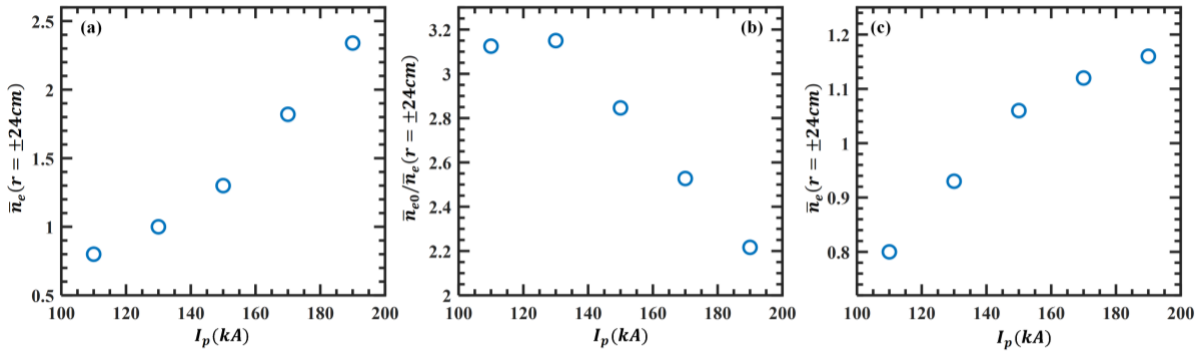

Figure 6. Corresponding to the same discharges in Fig.5. The edge ($r = \pm 24cm$) line-average electron density (a), and the ratio of central line-average density to the edge one (b), at the point of the onset of the HFSHD front. (c) The edge ($r = \pm 24\ cm$) line-average electron density, at the point of central line-average density equals to $\bar{n}_{e0} = 2.5 \times 10^{19}\ m^{-3}$.

All discharges showed in Fig.5 and 6 are performed on the same day under similar experimental conditions. The plasmas are all fueled by continuous gas-puffing. The fueling speed remains constant in every single shot. The nose of the gas-puff is located at the bottom of plasma, meaning that the fueling source is in-out symmetrical. Therefore, to some extent, $\bar{n}_{e\_edge}$ reflects the quantity of particles at the edge and $\bar{n}_{e0}$ represents the total amount of fueling. Fig 6(c) shows $\bar{n}_{e\_edge}$ versus I_P, at the same central line-average density of $\bar{n}_{e0} = 2.5 \times 10^{19}\ m^{-3}$, which is smaller than the threshold of the HFSHD front onset. The results indicate that there are more particles at edge in larger I_P plasmas, if the fueling amounts are the same. Moreover, the relationship of $\bar{n}_{e\_edge}(\bar{n}_{e0} = 2.5)$~$I_P$ is very similar to the observed relationship of $n_{e,HFSHD}$~I_P showed in Fig.5(c). This implies that the amount of edge particles plays an important role in determining the density of the HFSHD front.

The above results show that the critical threshold for the formation of the HFSHD front increases with I_P and is related to the radial gradient. Both these observations suggest that the edge temperature might be the crucial parameter.

In addition, the HFSHD front appearance is always associated with strong edge density asymmetry between the HFS and LFS, as presented by Fig. 2 and 3. The HFS-LFS density asymmetry indicates that a significant parallel density gradient forms at the edge. According to the two-point model in P. C. Stangeby (page 18p in Ref. [17]), the collision parameter ($n_e L/T_e^2$) is an effective criterion to describe the parallel gradient. A parallel gradient will arise after the collision parameter exceeds a certain value. Picking out three shots with different I_P from Fig.5, the traces of HFS-LFS density asymmetry, with $\bar{n}_{e0}$ and $n_e L/T_e^2$ are presented in Fig.7 (a-c) and (d-f) respectively. Here, the $L = \pi q_a R$ is the connection length between HFS and LFS limiters, the $n_e = \bar{n}_e(\pm 24cm)$ is measured by the POLARIS, and the T_e is relative temperature at $r = 23.5cm$, measured by electron cyclotron emission (ECE). We have assumed the central temperature $T_{e0} = 800eV$ when $I_p = 150kA, \bar{n}_{e0} = 2 \times 10^{19} m^{-3}$. It is interesting that the HFSHD front appears at the similar value of the collision parameter, even though the three shots have quite different plasma current and density threshold. This experimental result suggests that the collisionality plays an important role in the formation of the HFSHD front. It should be noted that, the n_e and T_e used in collisionality calculation are parameters inside the LCFS, not the SOL region. That is because there are no measurements for SOL plasma on J-TEXT. And the appearance of HFSHD front is firstly detected by density measurement at $r = \pm 24cm$. So, it is reasonable to use the local parameters where we observe it. Even though the two-point model in Ref. [17] is usually used to describe the SOL plasma on divertor devices, our experimental results indicate that it indeed can also be applied in limiter plasmas inside the LCFS. Besides, the plasma horizontal position is almost symmetrical between the HFS and LFS limiter, and do not change shot by shot. And we have to point out that the formation of HFSHD front do not demand that the LCFS contact with the HFS limiter. Dedicated experiments have been performed on J-TEXT, to study the effects of plasma horizontal displacement on HFSHD front. When the plasma moves outwards and contact the LFS limiter, it is interestingly found that the HFSHD front still appears and even forms at a lower density threshold.

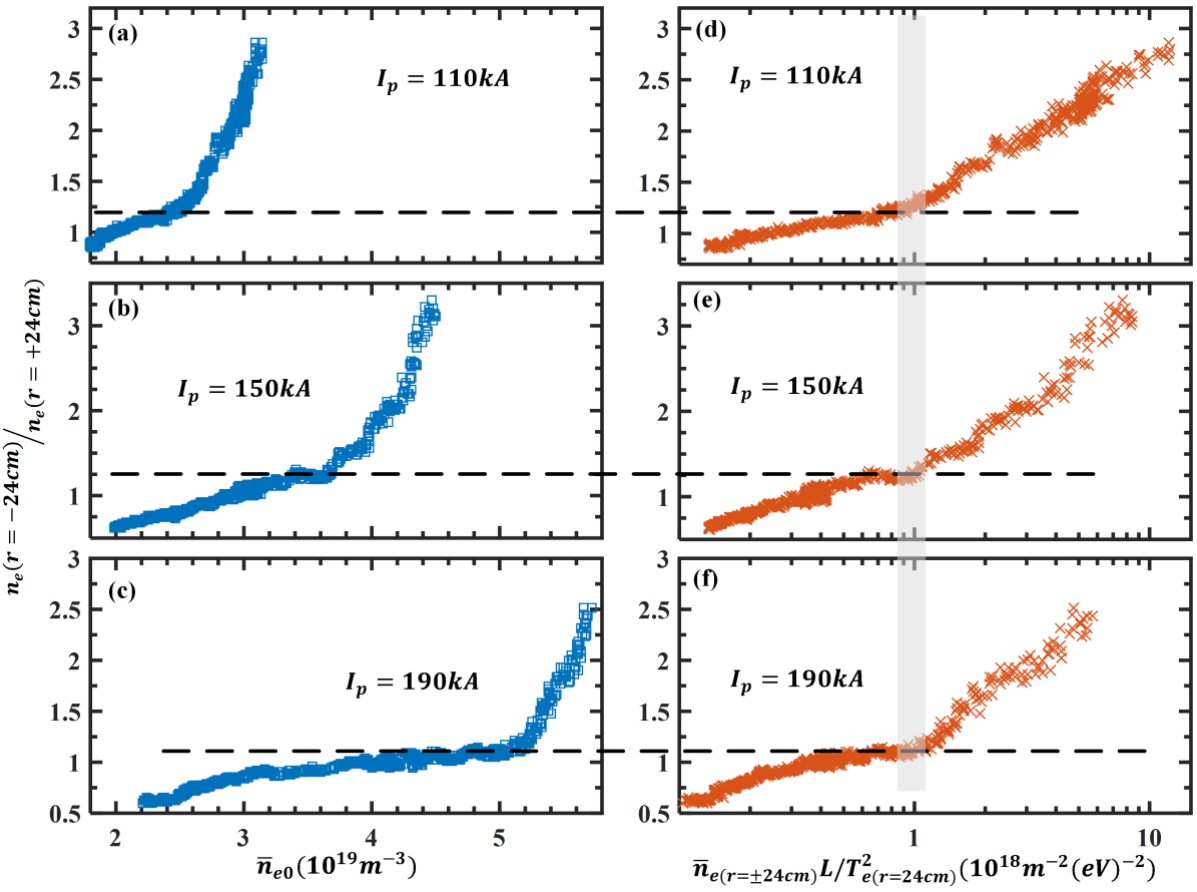

Figure 7. Traces of HFS-LFS density asymmetry against line-average density for (a) $I_P = 110\ kA$; (b) $I_P = 150\ kA$; and (c) $I_P = 190\ kA$ and against an edge collisionality parameter for (d) $I_P = 110\ kA$; (e) $I_P = 150\ kA$; and (f) $I_P = 190\ kA$.

5. Summary and discussion

The HFSHD front has been observed frequently for high density pulses in the limiter J-TEXT tokamak when plasma density reaches a threshold. Similar to observations on divertor devices [5-7], the high-density front forms at the scrape-off layer (SOL) on the high field side (HFS) and can be up to one order of magnitude larger than the separatrix density in the LFS region. The appearance of the HFSHD front leads to highly poloidally asymmetric distributions of electron density and impurity radiation. The evolution of the HFSHD front on J-TEXT exhibits two different phases with the continuous increase of density. In the first 'growing' phase, the HD front stays localized at the HFS edge as it grows in magnitude and extent. The high-density front seems stable and does not impact plasma confinement. As density reaches a certain value, the HFSHD front is found to move quickly poloidally during a second 'moving' phase. The motion of the high-density front appears to deteriorate plasma confinement rapidly and is usually observed to be followed by plasma disruption. This suggests that the HFSHD front may play an important role in setting the maximum achievable density on J-TEXT. The threshold density for the formation of the HFSHD front on J-TEXT is found to increases with plasma current. As all the discharges on J-TEXT are Ohmic heating only, the heating power depends broadly linearly with I_P. The results then are consistent with the observation on ASDEX-U that the density of the HFSHD front increases with total heating power [16]. Interestingly, different onset density for different discharges can be described by a common critical collisionality. This could be interpreted as the higher collisionality being beneficial for retention of the impurities and neutrals and, thus, increasing the ionization sources there.

Simulation of ASDEX Upgrade [7] shows that the recovery of the HFSHD front enables SOLPS modeling to solve some long-standing mismatching issues with experimental data of inner divertor plasma, such as divertor neutral density, neutral radiation levels and plasma fueling rates. The observation of the HFSHD front in a limiter device suggests that the existence of such consideration should be not restricted to machines with single null divertor configuration. Indeed, the high-density front seems more robust and has larger influence on plasma performance in J-TEXT. On J-TEXT, the plasma usually disrupts soon after the HFSHD front develops into the second 'moving' phase and the maximum achievable density is general well below the Greenwald density, $0.7n_G$. The formation and subsequent growth of the HFSHD front seems to set the machine operational limit. On ASDEX Upgrade, both simulation [7] and spectroscopic measurements [18] show that strong volumetric recombination starts to appear as the density increases, reducing the density in the inner divertor. The strong volumetric recombination provides a local plasma sink and stabilizes the growth of the HFSHD front. However, such a recombination sink is not expected to be significant in a limiter machine due to the lack a closure structure near the limiter target. Lack of a significant recombination sink could be the possible explanation of the more robust high-density front in HFS region.

In summary, the first observation of the HFSHD front in a limiter machine sheds a new light on the understanding of its SOL physics and provided a further challenge for modeling. Experimental and theoretical studies of the existence and phenomenology of the HFSHD front should not be limited to single null divertor devices. It also suggests that additional mechanisms should be considered to explain the formation and developing of the HFSHD front, apart from the self-amplifying process due to divertor structure and poloidal and perpendicular $E \times B$ drifts in the divertor.

Acknowledgement: This research is partly supported by National Magnetic Confinement Fusion Energy R&D Program under Grant No.2018YFE0310300 and the National Natural Science Foundation of China under Grant Nos. 11905080 & 11905050. This work is also partially funded by the RCUK Energy Programme (Grant No. EP/T012250/1).

Reference:

[1] ITER Physics Expert Group on Divertor, Chapter 4: Power and particle control, Nucl. Fusion **39** (12) (1999) 2391–2469, doi: 10.1088/0029-5515/39/12/304.

[2] M. Shimada, D.J. Campbell, V. Mukhovatov, M. Fujiwara, N. Kirneva, K. Lackner, M. Nagami, V.D. Pustovitov, N. Uckan, J. Wesley, N. Asakura, A.E. Costley, A.J.H. Donné, E.J. Doyle, A. Fasoli, C. Gormezano, Y. Gribov, O.

Gruber, T.C. Hender, W. Houlberg, S. Ide, Y. Kamada, A. Leonard, B. Lipschultz, A. Loarte, K. Miyamoto, V. Mukhovatov, T.H. Osborne, A. Polevoi, A.C.C. Sips, Chapter 1: Overview and summary, Nucl. Fusion **47** (6) (2007) S1–S17, doi: 10.1088/0029-5515/47/6/S01.

[3] Y. Wan, J. Li, Y. Liu, X. Wang, V. Chan, C. Chen, X. Duan, P. Fu, X. Gao, K. Feng, S. Liu, Y. Song, P. Weng, B. Wan, F. Wan, H. Wang, S. Wu, M. Ye, Q. Yang, G. Zheng, G. Zhuang, Q. Li, Overview of the present progress and activities on the CFETR, Nucl. Fusion **57** (10) (2017) 102009, doi: 10.1088/1741-4326/aa686a.

[4] K. McCormick, R. Dux, R. Fischer, A. Scarabosio, Main chamber high recycling on ASDEX upgrade, Journal of Nuclear Material **390-391** (2009) 465-469, doi: 10.1016/j.jnucmat.2009.01.145.

[5] S. Potzel, M. Wischmeier, M. Bernert, R. Dux, H.W. Müller, A. Scarabosio, ASDEX Upgrade Team, A new experimental classification of divertor detachment in ASDEX Upgrade, Nucl. Fusion **54** (1) (2014) 013001, doi: 10.1088/0029-5515/54/1/013001.

[6] P. Manz, S. Potzel, F. Reimold, M. Wischmeier, ASDEX Upgrade Team, Stability and propagation of the high field side high density front in the fluctuating state of detachment in ASDEX Upgrade, Nucl. Mater. Energy **12** (2017) 1152–6, doi: 10.1016/j.nme.2016.10.002.

[7] F. Reimold, M. Wischmeier, S. Potzel, L. Guimarais, D. Reiter, M. Bernert, M. Dunne, T. Lunt, The high field side high density region in SOLPS-modeling of nitrogen-seeded H-modes in ASDEX Upgrade, Nucl. Mater. Energy **12** (2017) 193–9, doi: 10.1016/j.nme.2017.01.010.

[8] M.G. Dunne, S. Potzel, F. Reimold, M. Wischmeier, E. Wolfrum, L. Frassinetti, M. Beurskens, P. Bilkova, M. Cavedon, R. Fischer, B. Kurzan, F.M. Laggner, R.M. McDermott, G. Tardini, E. Trier, E. Viezzer, M. Willensdorfer, The EUROfusion MST1 Team and The ASDEX-Upgrade Team, The role of the density profile in the ASDEX-Upgrade pedestal structure, Plasma Phys. Control. Fusion **59** (1) (2017) 014017, doi: 10.1088/0741-3335/59/1/014017.

[9] T.H. Osborne, G.L. Jackson, Z. Yan, R. Maingi, D.K. Mansfield, B.A. Grierson, C.P. Chrobak, A.G. McLean, S.L. Allen, D.J. Battaglia, A.R. Briesemeister, M.E. Fenstermacher, G.R. McKee and P.B. Snyder, Enhanced H-mode pedestals with lithium injection in DIII-D, Nucl. Fusion **55** (6) (2015) 063018, doi: 10.1088/0029-5515/55/6/063018.

[10] R. Maingi, D.P. Boyle, J.M. Canik, S.M. Kaye, C.H. Skinner, J.P. Allain, M.G. Bell, R.E. Bell, S.P. Gerhardt, T.K. Gray, M.A. Jaworski, R. Kaita, H.W. Kugel, B.P. LeBlanc, J. Manickam, D.K. Mansfield, J.E. Menard, T.H. Osborne, R. Raman, A.L. Roquemore, S.A. Sabbagh, P.B. Snyder and V.A. Soukhanovskii, The effect of progressively increasing lithium coatings on plasma discharge characteristics, transport, edge profiles and ELM stability in the National Spherical Torus Experiment, Nucl. Fusion **52** (8) (2012) 083001, doi: 10.1088/0029-5515/52/8/083001.

[11] S. Saarelma, A. Järvinen, M. Beurskens, C. Challis, L. Frassinetti, C. Giroud, M. Groth, M. Leyland, C. Maggi and J. Simpson, The effects of impurities and core pressure on pedestal stability in Joint European Torus (JET), Phys. Plasmas **22** (5) (2015) 056115, doi: 10.1063/1.4921413.

[12] G. Zhuang, Y. Pan, X.W. Hu, Z.J. Wang, Y.H. Ding, M. Zhang, L. Gao, X.Q. Zhang, Z.J. Yang, K.X. Yu, K.W. Gentle, H. Huang, J-TEXT Team, The reconstruction and research progress of the TEXT-U tokamak in China Nucl. Fusion **51** (9) (2011) 094020, doi: 10.1088/0029-5515/51/9/094020.

[13] G. Zhuang, J. Chen, Q. Li, L. Gao, Z.J. Wang, Y. Liu, W. Chen, First results of the J-TEXT high-resolution 3-wave polarimeter-interferometer system, Journal of Instrumentation, 8 (10) (2013) C10019, doi: 10.1088/1748-0221/8/10/C10019.

[14] M. Greenwald, Density limits in toroidal plasmas, Plasma Phys. Control. Fusion **44** (8) (2002) R27–R53, doi: 10.1088/0741-3335/44/8/201.

[15] S. Potzel, M. Dunne, R. Dux, L. Guimarais, F. Reimold, A. Scarabosio, M. Wischmeier, On the high density in the HFS far SOL at ASDEX Upgrade and its impact on plasma confinement, 42nd EPS Conference on Plasma Physics, Lisbon, Portugal, (2015).

[16] S. Potzel, M. Wischmeier, M. Bernert, R. Dux, F. Reimold, A. Scarabosio, S. Brezinsek, M. Clever, A. Huber, A. Meigs, M. Stamp, Formation of the high density front in the inner far SOL at ASDEX Upgrade and JET, Journal of Nuclear Material **463** (2015) 541-545, doi: 10.1016/j.jnucmat.2014.12.008

[17] P.C. Stangeby, The plasma boundary of magnetic fusion devices (Bristol; Philadelphia: Institute of Physics Pub), 2000.

[18] F. Reimold, M. Bernert, A. Kallenbach, B. Lipschultz, G. Meisl, S. Potzel, M.L. Reinke, M. Wischmeier, D. Wünderlich, The X-point radiation regime in detached H-Modes in full-tungsten ASDEX Upgrade, 42nd EPS Conference on Plasma Physics, Lisbon, Portugal, (2015).